ISSN: 0067-2904

Novel Nano Zn^{+2}-Compound from LA Ligand as an Acid-Base Indicator: Synthesis, Characterization, pH Sensor, and Fluorescent Study

Wafaa Waleed AL-Qaysi*, Alyaa Khider Abbas
Department of Chemistry, College of Science, University of Baghdad, Al-Jadriya Campus, 10071 Baghdad, Iraq

Received: 4/2/2023 Accepted: 5/6/2023 Published: 30/11/2023

Abstract

The main goal of our research is to synthesize a novel nano Zn^{+2} complex with the 8-(2-(dansyl chloride)azo)adenine (LA) ligand as a pH sensor because of its advantageous properties. The molecular formulas of the ligand and Zn^{+2}-LA complex were confirmed by studying the elemental analyses (C.H.N.), spectral methods, XRD, and thermal analyses (TGA). The molar ratio of Zn^{+2}-LA was studied as a ratio (1:2) (M:L). Through the survey in FT-IR and UV-Vis spectra, it was found that the complex has a tetrahedral geometry shape with a dark purple color λ_{max} (552 nm), obtained from a single molecule. The optimum concentration is 0.3 mM, pH = 5.5, and time = 0-3 hours, which in the studies followed Lambert-Beer's law. Linearity ranged from 0.025 to 0.4 mM for the Zn^{+2}-LA complex, with a linear correlation coefficient of 0.9963. The detection limit was 0.0219 µg/mL, and the limit of quantification was 0.0663 µg/mL. LA could be used as a titration indicator of sodium hydroxide (NaOH) by oxalic acid ($H_2C_2O_4$) with a maximum concentration of 0.1 M of $H_2C_2O_4$. Finally, the characteristic fluorescence peaks of the solutions were identified at 462 nm and 554 nm for the ligand LA and its complex respectively, which were dependent on pH = 5.5 and at 1 minute. The type of emission fluorescence is $\pi* \rightarrow n$ transition.

Keywords: Adenine azo ligand, Fluorescent, pH sensors, Zinc complexes.

مركب نانوي جديد من ايون الزنك الثنائي مع الليكند كدليل قاعدة– حامضية: تحضيره و خصائصه و دراسة كمستشعر الأس الهيدروجيني و الفلورة

وفاء وليد القيسي ، علياء خضر عباس

قسم الكيمياء، كلية العلوم ، جامعة بغداد، بغداد، العراق

الخلاصة

الهدف الرئيسي من الدراسة الحالية هو تحضير مركب نانوي جديد من ايون الزنك الثنائي مع الليكند 8–(2–(dansyl chloride)azo) adenine (LA) كمستشعر للاس الهيدروجيني pH بسبب خصائصه المفيدة التي تم الحصول عليها من جزيء واحد. الصيغة الجزيئية لليكند (LA) و معقد (Zn^{2+}–LA) تم تشخيصهم من خلال دراسة تحليل العناصر (C.H.N.) و الطرق الطيفية و تشتت الاشعة السينية و التحاليل الحرارية (TGA). النسبة المولية للمعقد (Zn^{2+}–LA) درست و كانت كنسبة (1:2) (M:L) و من خلال الاستقصاء في اطياف (FTIR) و UV–Vis وجد ان المعقد يمتلك شكل هندسي رباعي السطو و له لون

*Email: wafa.w@sc.uobaghdad.edu.iq

بنفسجي غامق و طول موجي اعظم (λ_{max}) (552 nm). وكانت الظروف المثلى من تركيز 0.3 mM و الاس الهيدروجيني pH =5.5 و الثباتية عند الوقت 0–3 hrs و التي اتبعت قانون لامبرت بير، اذ تراوحت الخط 0.025–0.4 mM لمعقد الزنك الثنائي– لليكند، مع معامل الارتباط الخطي 0.9963. كان حد الكشف 0.0219 ميكروغرام / مل، و كان حدود القياس الكمي 0.0663 ميكروغرام / مل. و من الممكن استخدام الليكند LA كمؤشر معايرة لهايدروكسيد الصوديوم NaOH بواسطة حامض اوكزاليك $H_2C_2O_4$ مع أقصى تركيز لحامض اوكزاليك
0.1M $H_2C_2O_4$.وأخيرًا، تم تحديد قمم التألق المميزة للمحلول عند الاطوال الموجية 462 نانومتر و 554 نانومتر لليكند و معقده عند الرقم الهيدروجيني pH=5.5 ، و دقيقة واحدة. اذا كان نوع الانتقالات الالكترونية للفلورة ($\pi * \rightarrow n$).

1. Introduction

Acid-base indicators, also referred to as pH indicators, are weak acids or bases with a chromic halo that change their structural composition as the solution's pH changes. Such indicators should, in theory, be sharp visual shifts, selective, sensitive, stable, infrequently specific, and free from interference with the solution's constituents. Examples include color, luminescence, fluorescence, or the lowest possible concentration of turbidity. The presence of a pH indicator has no bearing on whether a chemical solution is acidic or alkaline when employed as a diluted solution [1]. Numerous signs can be found in nature. A natural pH indicator built from a variety of lichens is called litmus, for instance. Flowers and vegetables include anthocyanins, which serve as pH indicators, and carotenoids [2]. Several azo compounds, including methyl red, methyl orange, and congo red, exist in three tautomeric forms; each one has a unique hue and can transform from one shape to another based on the pH of the environment. As a result, they are employed as pH indicators. Methyl red turns red at pH values below 4.4, yellow at pH values above 6.2, and orange at pH values in the middle [3]. Methyl orange is typically employed in the titration of acids. It is colored yellow in basic media and red in acidic media [3]. Researchers in many different domains have extensively exploited this property for detecting pH levels; in analytical chemistry, it is employed to establish the end point of an acid-base titration [3] and calculate the acidity of the living medium for biological research [4]. Additionally, azo compounds have been thoroughly studied in applications like inkjet printing and optical recording mediums due to their superior thermal and optical properties, oil-soluble light-fast dyes [5], organic photoconductors [6], and molecular memory storage [7]. Recent studies have found a tremendous increase in interest in identifying the most extensively used azo compounds as markers due to the existence of delocalization and hues, especially yellow, red, and orange. Organic azo compounds such as *p*-dibenzothiophen azo-8-naphthol derivatives [8] is are colorless to orange in basic media and from orange to colorless in acidic media, and the pH range of color change was (6-10); mercurial azo compounds [9], 1,8-naphthalimide derivatives [10], azo ligands as 2-amino-6-ethoxybenzothiazole and 4-chloro-3,5-dimethyl phenol derivatives [11], 3,4-dihydroxyazobenzene (DHAB), 4'sulfo3,4dihydroxyazobenzene (SDHAB), calcon (mordant black 17, CLN), 4-(thiazolylazo)resorcinol (TAR), 4(2thiazolylazo) 5 diethyl maminophenol (TAAP) azo compounds [12], 8-[5-(2-sulfonic acid naphthyl)azo] Caffeine (SNAC) is brown in acidic medium and red in basic medium [13], [4-(5-(7-Bromo-8-hydroxyquinoline)azo)sulfamethoxazole] (HAS) is orange in acidic medium and red in basic medium [14], and 2-((9H-prin-6-yl)diazenyl)-5-(dimethylamino) naphthalene-1-slfonyl chloride (DAD) is purple color in basic medium and yellow color in acidic medium [15], and for the fluorescence spectroscopic analysis [16], sensor activity of three *N*-phthalimide azo-azomethine derivatives toward metal ions in environmental water samples [17], an azo dye (*E*)-1-((5-methoxythiazolo[4,5-b]pyridin-2-yl)diazenyl)naphthalen-2-ol (TPN1) based sensor

in a purple color dye for selective and sensitive detection of Cu^{+2}, Sn^{+2}, and Al^{+3} ions [18]. In our work, novel nano Zn+2- LA complexes will be synthesized and characterized by spectroscopic techniques (FT-IR, UV-Vis, and ^1H NMR), thermal analysis (TGA), elemental analysis (C.H.N), XRD, and molar conductivity, before investigation of their dyeing properties, antioxidants, and anticancer applications.

2. Experimental

2.1. Materials

All chemicals ($ZnCl_2$, $NaNO_2$, HCl, Adenine, Dansylchoride, and Ethanol) were obtained from Sigma Aldrich and used without further purification.

2.2. *Chemistry*

2.2.1. Synthesis of [8-(2-(dansyl chloride)azo)adenine] (LA) ligand

In a round-bottomed flask**,** adenine (1 mmol) and sodium nitrite solution (15 mL, 10%) at 0-5 °C were stirred for 30 minutes to afford the diazonium salt of adenine. This salt was then slowly added with continuous stirring to the cooled basic solution of adansyl chloride, which was used as a coupling reagent. The solid crude material was then filtered, washed with ethanol and water several times, and dried to give the desired ligand [19].

2.3. Synthesis of Zn^{+2}-LA complex

A solution of the ligand (0.002 mol) in a minimal amount of ethanol was slowly added to a stirred $ZnCl_2$ solution (100 mL, 0.001 mol/L). The reaction mixture was then stirred until a deep violet-colored precipitate was formed. The solid crude material was then filtered, washed several times with ethanol and water, and dried in air to give the Zn^{+2}-LA complex (Scheme 1) [14].

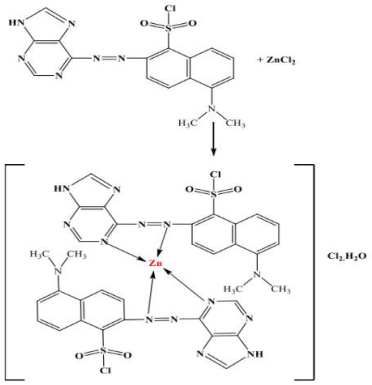

Scheme 1: Synthesis of Zn^{+2}-LA complex

2.4. Statistical analysis

The data were presented as averages, and the standard deviation (SD) was gathered from studies done in triplicate. Data were evaluated using the "Origin 5.0" ANOVA to analyze differences, and significance was shown at $p<0.005$ [15].

3. Results and discussion

Dansyl chloride and adenine were used to synthesize a novel azo ligand (LA) over a reaction (diazo-coupling). This ligand was reacted with $ZnCl_2$ to form a Zn complex. The results taken from elemental analysis and magnetic susceptibility for the LA and Zn^{+2}-LA complex satisfying approval with calculated values are shown in Table 1. The proposed structural formula for the ligand (LA) and the Zn^{+2}-LA complex was confirmed by the microelemental analysis (C.H.N), magnetic moment, thermal gravimetric analysis (TGA), and molar conductivity measurements; however, the Zn^{+2}-LA complex has an ionic character with

a (1:2) electrolyte. Also, the synthesized compounds become stale with time (Figure 1). Unaffected by the atmosphere and moisture, as well as being dissolved in ethanol, methanol, DMSO, and DMF.

Table 1 : Some physicochemical properties and elemental analysis of the ligand and Zn^{+2}- LA complex

Compound (M.wt) g/mol	M:L	Color $\lambda_{(nm)}$	Elemental analysis Found (%)						Λ_m m.S.mol^{-1} .cm^2(EtoH)	m.p. (°C)
			C	H	N	S	M	Cl		
(LA) $C_{17}H_{14}N_7O_2ClS_2$ (415.92)		Orange 464	49.34 (49.04)	4.01 (3.36)	23.85 (23.56)	7.88 (7.69)	-	-	-	138-140
$[Zn(C_{17}H_{14}N_7O_2ClS)_2]CL_2.H_2O$ (986.22)	1:2	Deep purple 552	41.89 (41.37)	3.72 (3.04)	20.01 (20.01)	6.88 (6.88)	7.02 (6.62)	14.91 (14.39)	15	90-92

3.1. FT-IR spectroscopy

The identification vibration bands of the free ligand (LA) and Zn^{+2}-LA complex were compared. The FT-IR spectrum of the ligand (LA) was compared to the Zn^{+2}-LA complex spectrum in order to confirm the cheating mode with the LA to the Zn^{+2} in the complex. The FT-IR spectrum of the ligand (LA) showed two absorption bands at 1598 and 1620 cm^{-1} belonging to the C=N group at the pyrimidine ring (Figure 1). This band was then shifted to lower frequencies (1614 cm^{-1}) in the spectrum of Zn^{+2}-LA complex, with sharpness due to the chelating of the zinc with nitrogen atoms (Figure 2) [20]. The most characteristic band in the LA spectrum is for the N=N group, which appeared at 1436 and 1402 cm^{-1}, and with chelating to Zn^{+2}, these bands changed to 1442 and 1409 cm $^{-1}$[21]. The other absorption bands, such as N-H and SO_2Cl, were not unaltered in shape and position, which is a good indication of their nonparticipation in the chelation with Zn^{+2}. The FT-IR spectrum of Zn^{+2}-LA complex revealed new bands at 503 and 508 cm -1attributed to the M-N (Zn^{+2} with an azo group) and M-N (Zn^{+2} with a pyrimidine ring), respectively [22,23]. From these results, we can conclude that the ligand LA behaves neutrally as *N*,*N*-bidentate. All the details of the FT-IR spectral data for the ligand complex are shown in Table 2.

Table 2 : Diagnostic FT-IR bands (υ, cm $^{-1}$) for the ligand (LA) and Zn^{+2}-LA complex

Compound	C=N Pyrimidine	N=N Azo	N-H Imidazole	SO_2Cl	M-N (Zn-N_{azo})	M-N (Zn-$N_{pyrimidine}$)	M-Cl
LA	1620 1598	1436 1402	3460	1203	-	-	-
Zn^{+2}- LA	1614	1442 1409	3454 3419	1209	503	580	-

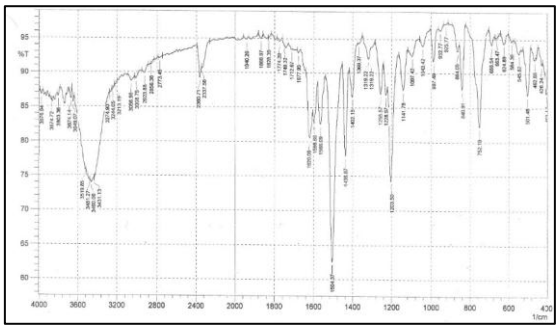

Figure 1: FT-IR spectrum of the ligand (LA)

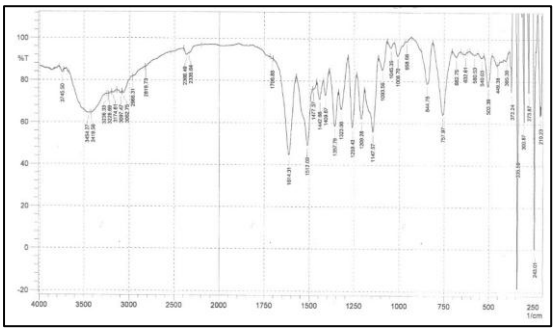

Figure 2 : FT-IR spectrum of the Zn^{+2}-LA complex

3.2. Thermogravimetric analysis (TGA)

The thermal decomposition behavior of the ligand (LA) and Zn^{+2}-LA complex was discussed by the thermogravimetric technique. The TGA thermograms are shown in Figures 3 and 4, while the outcomes are listed in Table 3. Generally, the ligand and its complex display for steps in the range 25-800 °C with argon gas. For the Zn^{+2}-LA complex, the first step of decomposition started at 25 °C and ended at 50 °C with a corresponding weight loss of 2.90%, which is in indication of the presence of lattice water. The second stage of decomposition was noticed at temperatures ranging from 50 to 285 °C (25.96% weight loss). The third and fourth stages of decomposition lost weights of 25.96 (285-590 °C) and 9.12% (590-800 °C), respectively. The Zn^{+2}-LA complex is more thermally stable than the ligand (LA) due to the complex residue (35.41%), while the residue of the LA ligand is 5.29% [15,24].

Table 3 : TGA data for the ligand (LA) and Zn^{+2}-LA complex

Compounds	Molecular formula and M.wt (gm/mole)	Stage	TGA range of the decomposition (°C)	Proposed assignment	Calculated (%)	Experimental (%)
LA	$C_{17}H_{14}N_7O_2ClS$ (415.92)	1	25-325	$C_{14}H_5$	41.59	41.97
		2	325-400	$C_3H_9Cl_{0.4}$	14.26	14.83
		3	400-625	$Cl_{0.6}N_7S$	36.45	35.65
		4	625-1000	O_{0-5}	1.192	1.189
		residue	>1000	O_{1-5}	5.77	5.29
$[Zn(LA)_2]Cl_2.H_2O$	$ZnC_{34}H_{30}O_5Cl_4$ (986.22)	1	25-50	$H_{12}O$	2.83	2.90
		2	50-285	$C_{21}H_{15}$	27.07	26.61
		3	285-590	$C_{13}H_3Cl_{0.4}$	26.92	25.96
		4	590-800	ClN_4	9.27	9.12
		residue	>800	$ZnN_{10}O_5S_2$	35.41	35.41

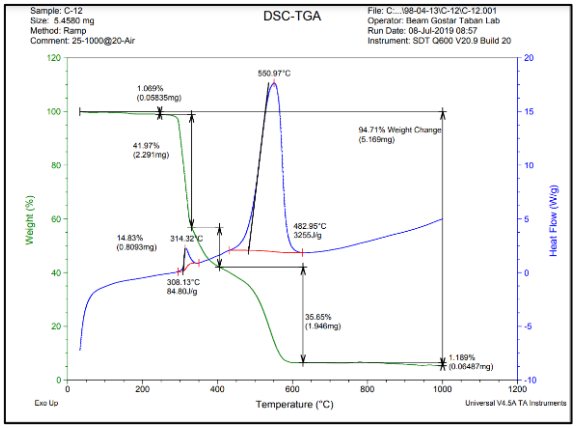

Figure 3 : TGA thermogram of the ligand

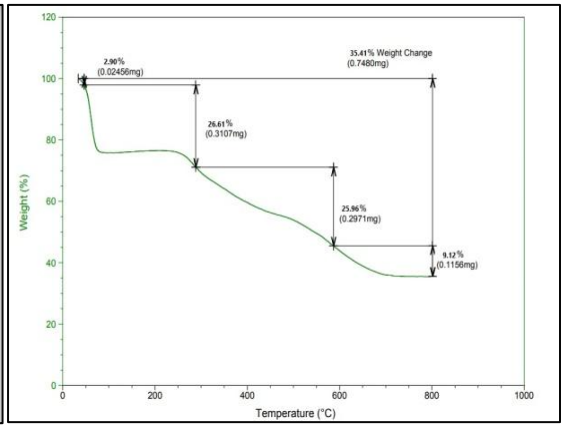

Figure 4 : TGA thermogram of the Zn^{+2}- LA complex

3.3. Scanning electron microscopy analysis (SEM)

The forms of the surface for the Zn^{+2}-LA complex were confirmed by the studying SEM technique. Figure 5 displays the SEM image for the complex, which is non-uniform with a smooth surface and coral shape (D = 53.83 nm). The image tends to be white, which indicates the large molecule [25].

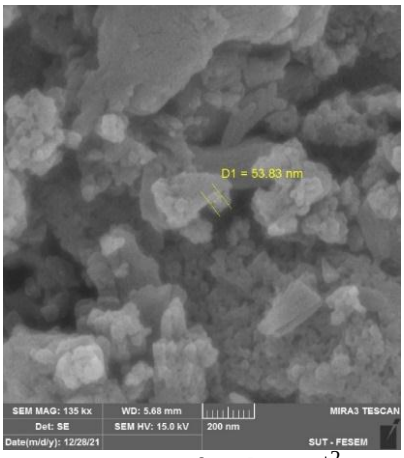

Figure 5 : SEM image for the Zn^{+2}-LA complex

3.4. X-Ray diffraction (XRD) analysis

The X-ray diffraction patterns in the range $5 \leq 2\theta \leq 65$ (for the LA ligand and Zn^{+2}-LA complex with an X-ray source crystal (CuKu), which was examined, indicated the degree of crystallinity of these compounds. Figures 6 and 7 showed the three strongest reflection peaks for the LA ligand and Zn^{+2}-LA complex in the range of 2θ (11.3495-13.971) and (11.3491-16.5335), respectively. The main characteristic reflection peak for the LA ligand occurs at 11.3491, and the band at 16.5335 is for Zn^{+2}-LA complex. According to this information, the semi-crystalline nature and particle size of the LA ligand and Zn^{+2}-LA complex were estimated from XRD patterns based on the highest intensity value compared with the other bands employing the renewed Debye-Scherrer equation ($D = (k\ \lambda/\beta \cos\theta)$ [26], where D is the mean size of crystalline domains, which may be equal to or smaller than the crystal grain size (the apparent particle size of the grains) and was represented as volume function by A or nm unit. K is a constant that represents a factor without unit and typical value at a bout (K = 0.94), λ is the X-ray wavelength (0.15406 nm), β is the full width at half maximum (FWHM) of the X-ray diffraction peak, whereas θ is the Bragg angle. The particle sizes of the LA ligand and Zn^{+2}-LA complex are 0.1679 and 0.3480 nm, respectively. These values emphasize that the particle size is located within the nanoscale range [27]. The interplanar spacing (d) was calculated from the status of the intense peak according to Brag's equation ($n\lambda = 2d \sin\theta$). Where $\lambda = 1.5406\ A^0$; n = an integer number]. The d dot was calculated and observed in the LA ligand at 7.781; 7.790 Å, and in the Zn^{+2}-LA complex at 5.355; 5.357 Å.

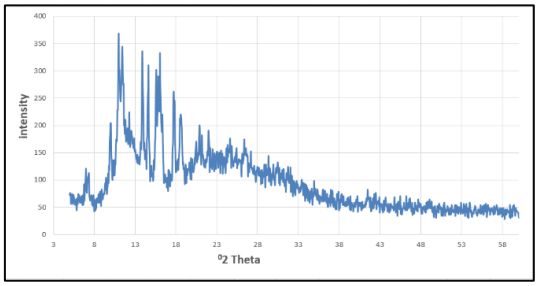

Figure 6 : X-Ray diffraction of the LA ligand

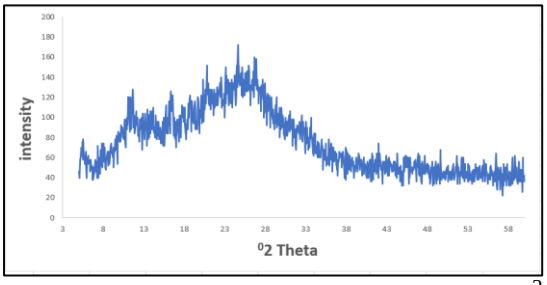

Figure 7 : X-Ray diffraction of the Zn^{+2}-LA complex

3.5. Electronic absorption spectra and magnetic moment measurements

The azo ligand (LA) and Zn^{+2}-LA complex were examined in the UV-Vis range. The free ligand appeared at $n \rightarrow \pi^*$ transition due to intramolecular charge transfer of heterocyclic and the aromatic moieties were assigned at 462 nm (21645 cm^{-1}) [28]. The electronic spectrum of

Zn^{+2}-LA complex showed a shift towards a high wave length of the absorption band at 554 nm (18050 cm^{-1}) and conformed the chelating of the ligand (LA) to the Zn^{+2} (Figure 8) [29].

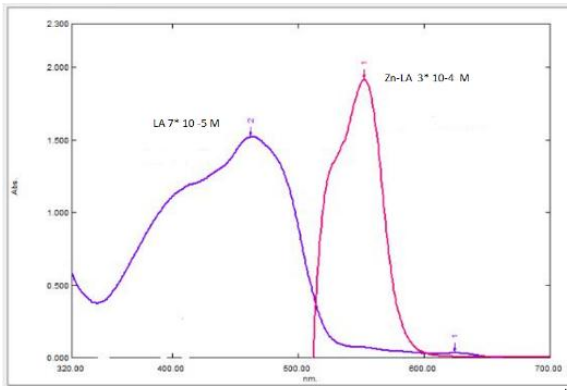

Figure 8 : The UV-Vis spectrum of the LA ligand and Zn^{+2}-LA complex

3.6. Optimization of experimental conditions for the Zn^{+2}-LA complex

The complex's optimum performance was attained using a variety of experimental settings, including pH reaction, concentration of the Zn^{+2}-LA complex, and time. The studies' pH was controlled using the Briton-Robinson buffer (BR) during this process. The results of interference investigations showed that when there is a Zn^{+2}-LA and BR buffer solution, less interference is present. But in the absence of Zn^{+2}, the LA pH values had no impact on the hue's transition to yellow [15]. The Zn^{+2}-LA solutions displayed a deep purple color, and the peaks in the absorption spectra were visible at 554 nm using the BR buffer solution with a pH range of 2-5.5 and for the LA ligand at 464 nm. The hue of the solutions was unaffected by changing the BR buffer solution, and thus for further studies. The BR buffer solution specified a concentration of 40 mM. The Zn^{+2} salt is mixed immediately with the LA ligand at 25 °C to synthesize Zn^{+2}-LA complex, and the maximal absorbance of the substance is 554 nm, as shown in Figure 9. The dark purple color gets more intense at pH 5.5.

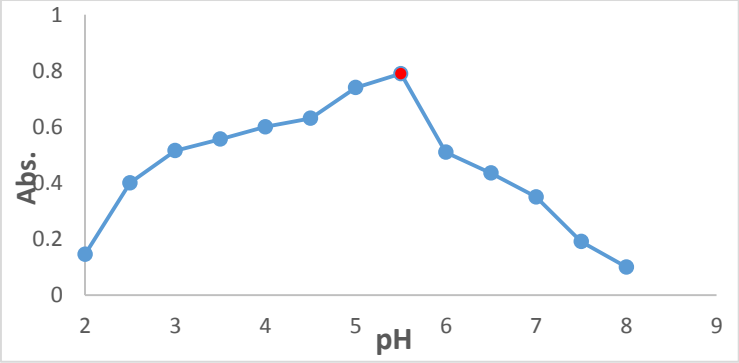

Figure 9 : The effects of pH buffer solutions on the color development of Zn^{+2}-LA complex 0.3 mM, BR buffer solution 40 mM, and 25 °C at 0 minutes

As shown in Figure 10, estimating the optimal concentration for the Zn^{+2}-LA complex is necessary. As anticipated, the reaction was failed when the Zn^{+2}-LA combination present at a lower concentration (less than 0.02 mM), which reduced the sensitivity of the Zn^{+2}-LA complex. When the concentration of the Zn^{+2}-LA complex is greater than 0.025 mM, as procedure becomes increasingly sensitive, and the developed solution's color deepens. Therefore, the optimum Zn^{+2}-LA complex concentration was determined to be 0.3 mM. In the presence of various concentrations of Zn^{+2}-LA complex, under all ideal experimental settings,

systems for identifying colors in UV-Vis absorption spectra were used, and the solution's absorbance at 554 nm significantly increased with the concentration of Zn^{+2}-LA complex.

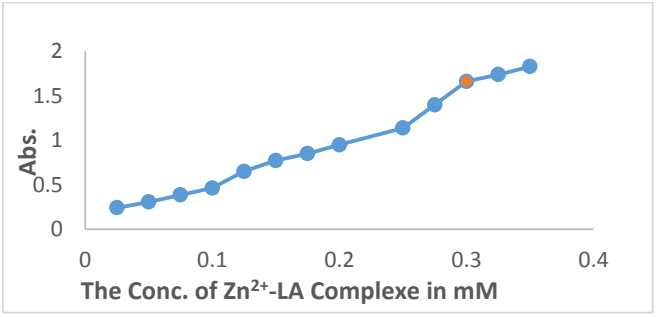

Figure 10 : The effects of the concentrations on color development of the Zn^{+2}-LA complex, 0.025-0.35 mM, pH = 5.5, 40 mM BR buffer solution and 25 °C at 0 minutes

The solution's color gradually changed from yellow to deep purple. With the bare eye, it is easy to see how the solution's color changes (i.e. the experiment's visual limit) when the concentration of Zn^{+2}-LA complex is higher than 0.025 mM. For speedy and portable colorimetric detection, it was also necessary to take the Zn^{+2}-LA complex reaction time into account. The proposed methodology's accuracy and repeatability are impacted by the response temperature's tendency to degrade, which was chosen at 25 °C. Figure 11 showed that the Zn^{+2}-LA complex reaction timings were completed more quickly than it would have taken for the reaction to finish.

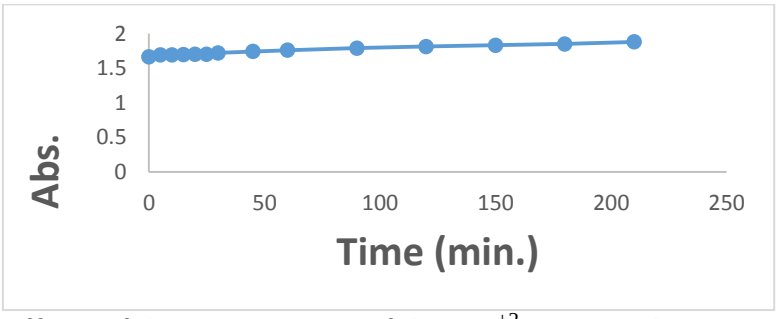

Figure 11 : The effects of the reaction time of the Zn^{+2}-LA complex, 0.3 mM, pH = 5.5, 40 mM BR buffer solution, and 25 °C at 0-250 minutes

3.7. The analytical performance for the Zn^{+2}-LA complex

The Zn^{+2}-LA complex solution's absorbance at 554 nm increased noticeably as the Zn^{+2}-LA complex concentration increased from 0.025-0.35 mM. The outcome was that the color of the solution progressively shifted from yellow to deep purple. With the bare eye, it is easy to see how the solution's color changes (i.e., the experiment's visual limit) when the Zn^{+2}-LA complex concentration is higher than 0.025 mM. Absorption of the Zn^{+2}-LA complex with excellent linearity with LA concentrations was seen at 554 nm in the range of 0.025-0.35 mM, as shown in Figure 12.

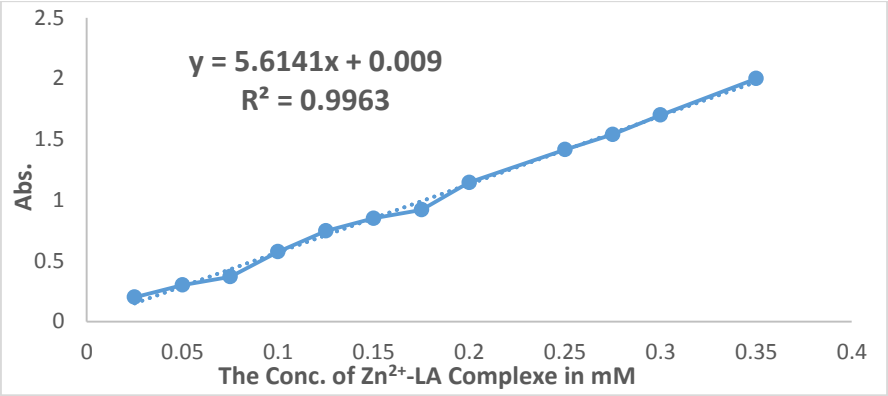

Figure 12 : The colorimetric methods successfully used all of the ideal conditions to achieve the linear calibration curves for Zn^{+2}-LA complex determination, 0.025-0.35 mM for the Zn^{+2}-LA complex at 25°C, 0 minutes, pH 5.5, and 40 mM BR buffer solution.

The resulting regression equation was: A 554 = with a correlation coefficient (R^2) of 0.9963, where x is the concentration expressed in mM units. The limits of detection (LOD) were determined using the formulas (3.3σ/S) in mM, and quantification (LOQ) was determined using the formulas (10σ/S) in M, where S is the regression equation's slope and σ is the intercept's standard error. By measuring the relative standard deviation (RSD), the reproducibility of the Zn^{+2}-LA complex was confirmed, and it was determined to be less than 3% at n = 5, demonstrating the method's excellent parameter. The concentration of the Zn^{+2}-LA complex is 0.3 mM, which shows very good repeatability and reproducibility, as shown in Figure 10. For the suggested methods, all regression equation statistics are given in Table 4.

Table 4 : The linear regression lines' summary statistic for determining the Zn^{+2}-LA complex

Parameter	Zn^{+2}-LA complex
Linearity (M)	0.025-0.35 mM
Regression	3.76086714
equation	5.6141x + 0.009
Slope	5.6141 ± 0.0002
Intercept	0.009
R^2	0.9963
r	0.9981
LOD	0.0219
LOQ	0.06638
Sensitivity	5.6141
σ	0.07446
SE (Standard Error)	0.021533971
SD (Standard Deviation)	0.07446

3.8. Proposition the mole ratio

Through the spectroscopic study of the solutions of mixing Zn^{+2} with LA ligand**,** the molar ratio method was applied by utilizing the optimal concentration (0.3 mM). Figure 13 shows the relationship that was obtained.

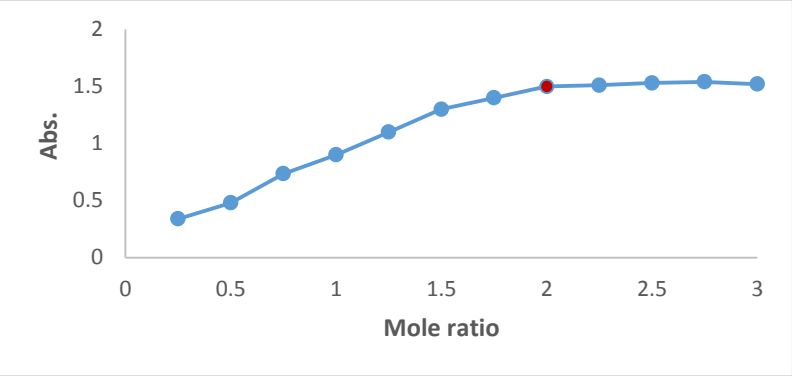

Figure 13 : The mole ratio of LA ligand and Zn^{+2}-LA complex while the data are listed in Table 5. The result indicates the formation of a M:L (1:2) ratio.

Table 5 : Absorbance of a LA-metal ion solution versus mole ratio

L:M	Absorbance
0.25	0.34
0.5	0.48
0.75	0.735
1	0.9
1.25	1.1
1.5	1.3
1.75	1.4
2	1.5
2.25	1.51
2.5	1.53
2.75	1.54
3	1.52

3.9. Stability constant and Gibbs free energy (ΔG)

To find the stability constant (K) for a Zn^{+2}-LA complex with a molar ratio of 1:2 of M:L, we follow the following equations [28].

$$K = \frac{(1-\alpha)}{4\alpha 3\ c2} \quad ; \quad \alpha = \frac{(Am - As)}{Am}$$

Where α = Degree of dissociation

C = Molar concentration for the complexes in molar (c = 0.3 mM)

Am = Absorbance of a solution containing an excess of ligand

As = Absorbance of a solution containing a stoichiometric amount of ligand and metal ions.

It was found that it possesses a high stability constant (K) (26.04×10^6 Mol^{-2}. L^2). The high value of (K) gave good information about the stability of the complex.

The Gibbs free energy (ΔG) can be calculated from this equation:

$\Delta G = - RT \ln K$

Where: R = gas constant, which equals 8.314 J. $mole^{-1}$. K^{-1}.

T = absolute temperature in Kelvin is 298.

ΔG for the Zn^{+2}-LA complex equals -42233.82 $J.mole^{-1}$.

This indicates that the reaction to synthesize the complex is thermodynamically spontaneous.

Based on the sharp color change from yellow to bright purple with indicator LA ligand examination, LA ligand will be further examined for acid-base titration indicator compounds. LA ligand will be tested for equivalent points in acid-base at pH 3-11.

3.10. Color stability test

Color stability was determined by measuring the discoloration time at an equivalent point in the titration. Since the pH range that causes a color shift for LA ligand titration is between 3 and 11, for the purpose of examining color stability at an equivalent point, we shall select the NaOH solution with $H_2C_2O_4$ solution at different concentrations. Table 5 contains the results of the color stability of the equivalent point for the titration of NaOH solution with $H_2C_2O_4$ solution. According to Table 6, the range of $H_2C_2O_4$ concentrations is from 0.025 to 0.5 M.

Table 6 : The analogous point for NaOH solution titrated by $H_2C_2O_4$ solution

Concentration (M)		Indicator (LA)	
$H_2C_2O_4$	**NaOH**	**Color Change**	**Color stability (minutes)**
0.025	0.025	Yellow to bright purple color	180
0.05	0.05	Yellow to bright purple color	180
0.1	0.1	Yellow to bright purple color	180
0.15	0.15	Yellow to bright purple color	180
0.2	0.2	Yellow to bright purple color	180
0.25	0.25	Yellow to bright purple color	180
0.5	0.5	Yellow to bright purple color	180

3.11. Applications of LA ligand as a titration indicator for acid-base

We shall contrast the use of the LA ligand as a titration indication with that of the reference indicator phenolphthalein during the titration of the NaOH solution with the $H_2C_2O_4$ solution (0.1 M). Figure 14 depicts the color change during titration, and Table 6 contains the results of the titration. According to Table 7, the target compound LA ligand can be used to titrate tacid-base with the same accuracy as phenolphthalein.

Table 7 : The results of $H_2C_2O_4$ solution (0.05 M) titration with NaOH using phenolphthalein and LA ligand as titration indicators

Indicator compounds	Color Change	Average Volume of $H_2C_2O_4$ solution (mL) ± S.D
LA	Yellow to bright purple	4.89 ± 0.003
Phenolphthalein	Pink to colorless	4.87 ± 0.003

Figure 14: Color change with indicator compound LA

3.12. Fluorescent spectra of compounds

The emission spectra of the LA ligand and the Zn^{+2}-LA complex were recorded in EtOH at room temperature, as seen in Figures 15 and 16, respectively. The ligand exhibits an excitation maximum wavelength at 462 nm and is characterized by an emission maximum (λ_{em}, max) at 700.723 nm and a low intensity (72.346 nm), which is shifted upon binding to metal ions. While the Zn^{+2}-LA complex has maximum fluorescence emission wavelengths (λ_{em},max) at 700.372 nm, excitation wavelengths at 552 nm show a strong and sharp intensity of 372.346, which is slightly red shifted when compared to the ligand. It also exhibited a broad peak at 536 nm with an intensity of 21.5, while the Zn^{+2}-LA complex exhibits long wavelengths at 667 nm with an intensity of 21.57, indicating that the ligand successfully chelated metal ions. The type of emission fluorescence is the $\pi* \rightarrow n$ transition.

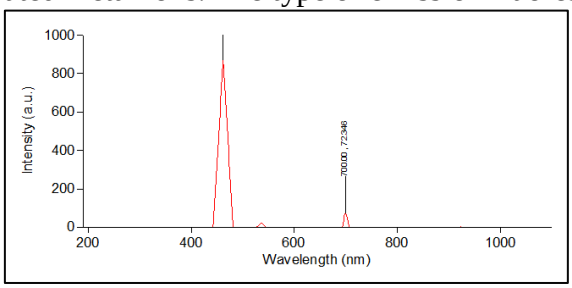

Figure 15 : Fluorescent spectra for the LA ligand in λ_{exc}= 462 nm

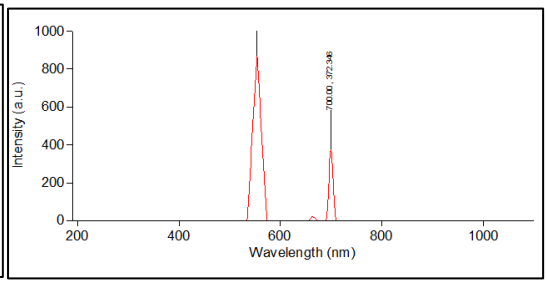

Figure 16 : Fluorescent spectra for the Zn^{+2}-LA complex in λ_{exc}= 552 nm

3.13. Dyeing properties

Azo dyes are highly colored and have been utilized as dyes and pigments for a long time [15]. The LA ligand and Zn^{+2}-LA complex on a wool fabric were applied. These dyes provided colors from orange to pomegranate (Figure 17), with good brightness and depth on fabric (Table 8). As well as standing, the color fastness of the textiles was examined for washing with soap powder at a concentration of 2%. So provided excellent fastness to both wet and dry robbing and excellent light fastness for defiled and color shift, all of this is subject to Iraqi standards for woolen textile No. 3616.

Table 8 : Dying properties of LA ligand and Zn^{+2}-LA complex

Compound	Color	Dry rubbing	Wet rubbing	Staining with dye	Color change
LA	Orange	3	3	3	4
Zn^{+2}-LA complex	Pomegranate	5	5	5	4

Grinding: 1-2 (not good), 3 (moderate), 5-4 (good) according to Iraqi specifications No. 3616 for woolen fabric.

Figure 17 : The fiber textile dyeing of LA ligand and Zn^{+2}-LA complex

3.14. Antioxidant Activity

Figures 18 and 19 depict the scavenging effect of LA ligand and the Zn^{+2}-LA complex at various doses. As they high inhibition power compared to ascorbic acid, which was used as a control. Five concentrations (12.55, 25, 50, 100, and 200 µg/mL) of the LA ligand and Zn^{+2}-LA complex were more effective in DPPH radical scavenging activity than ascorbic acid. Table 9 shows the scavenging activity that increased dramatically with increasing concentration.

Table 9 - Radical scavenging activity of the LA ligand, the Zn^{+2}-LA complex, and ascorbic acid.

Concentration (µg/mL)	DPPH Radical scavenging Activity (Mean ± SD)		
	Ascorbic Acid	**LA ligand**	**Zn^{+2}-LA complex**
12.5	46.01 ± 1.43	18.01 ± 1.8755	38.52 ± 0.799
25	52.47 ± 2.827	26.96 ± 4.513	41.16 ± 1.794
50	64.21 ± 4.914	41.83 ± 4.692	57.49 ± 1.261
100	74.82 ± 1.823	54.68 ± 3.001	66.92 ± 3.99
200	80.25 ± 2.981	75.81 ± 2.988	73.89± 1.989

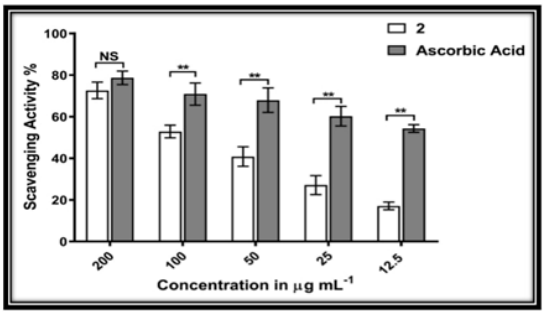

NS= No signal **= there is a sign

Figure 18 : Scavenging activity of the LA ligand

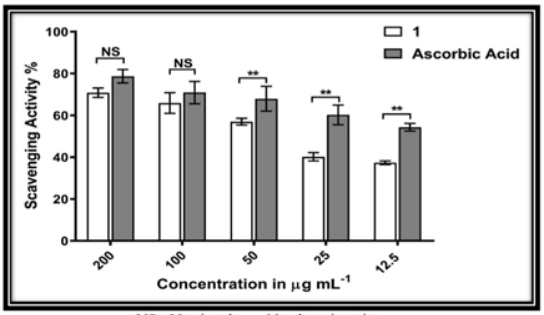

NS= No signal **= there is a sign

Figure 19 - Scavenging activity of the Zn^{+2}-LA complex

3.15. Study of the cytotoxic effects

The cytotoxic effectiveness and mechanism of behavior of the LA ligand and Zn^{+2}-LA complex were investigated against liver carcinoma cell lines (HepG-2) and normal cell lines (HdFn) by MTT assay after incubation for 24 hours at 37 °C with concentrations of 6.25-400 µg/mL. It was found that these compounds had different growth inhibitory effects on HepG-2 and HdFn cell lines. The data from Tables 10 and 11 and Figures 20 and 21 showed that the cell viability of the HepG-2 cell line was reduced by increasing the concentration of these compounds, but we notice the opposite in the case of the normal cell line (HdFn). It can be concluded that the greatest cytotoxic effect occurs at a concentration of 400 µg/mL. The half maximal inhibitory concentration (IC_{50}), which was utilized to measure drug efficacy, and also the p-value are used in hypothesis testing. The IC_{50} is lower; therefore, a lower concentration of drugs is required to stimulate carcinoma cell death and thus can be tolerated.

Table 10 : Inhibition effect of the LA ligand on HepG-2 and HdFn cell lines after incubation for 24 hours at 37 °C

Cell line	Concentration (µg /mL) (Mean and Std. Error of Mean)							IC_{50} (µg/mL)	p-value
	400	**200**	**100**	**50**	**25**	**12.5**	**6.25**	102	0.0001
HepG-2	52.28 ± 1.46	62.32 ± 2.97	72.46 ± 2.22	84.99 ± 3.99	94.99± 0.80	93.11 ± 6.33	95.55 ± 0.61		
HdFn	80.01 ± 1.90	83.98 ± 2.59	93.01 ± 0.50	94.99 ± 1.93	94.82 ± 2.70	94.30 ± 2.96	94.90± 1.89	57	

Table 11 : Inhibition effect of the Zn^{+2}-LA complex on HepG-2 and HdFn cell lines after incubation for 24 hours at 37 °C

Cell line	Concentration (µg /ml) (Mean and Std. Error of Mean)							IC_{50} (µg /mL)	p-value
	400	**200**	**100**	**50**	**25**	**12.5**	**6.25**		
HepG-2	42.98 ± 7.34	52.53 ± 1.43	55.14 ± 1.96	71.93 ± 7.90	85.34± 7.39	95.99 ± 1.01	94.69 ± 1.77	97	0.0001
HdFn	75.01 ± 1.09	83.99 ± 1.90	93.10 ± 2.29	93.99 ± 0.61	94.11 ± 1.39	95.13 ± 1.20	95.29± 1.13	28	

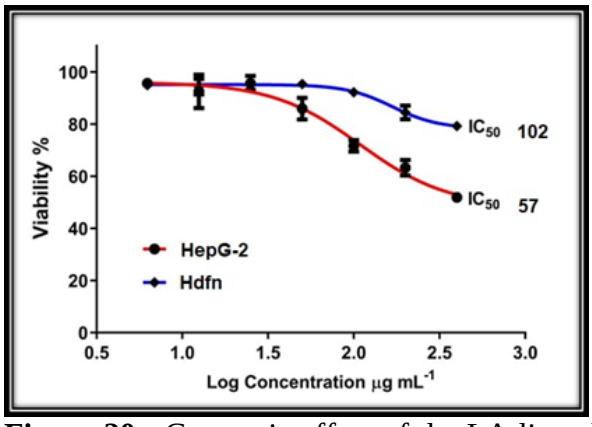

Figure 20 : Cytotoxic effect of the LA ligand

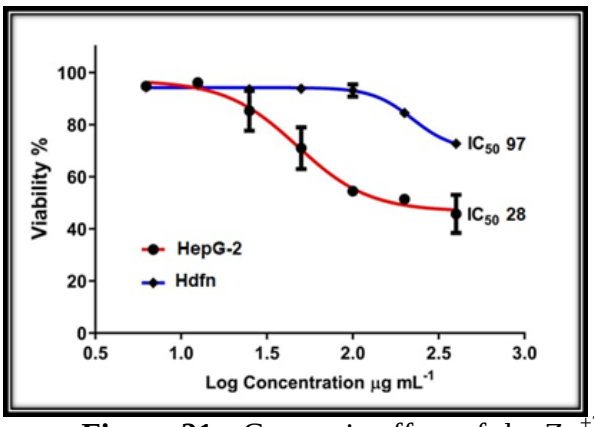

Figure 21 : Cytotoxic effect of the Zn^{+2}-LA complex

4. Conclusion

In this study, we demonstrate that a straightforward, economical, and precise novel nanoazo complex made up of Zn^{+2} ions with LA ligand works with a pH of 4. The LA might be utilized as a titration indicator instead of the phenolphthalein indicator for titration of NaOH with $H_2C_2O_4$ with the same result. Finally, we see a shift to a longer wavelength in complexes when compared with ligands, which indicates that the ligand successfully chelated metal ions.

References

[1] B. S. Bahl, A. Bahl, and G. D. Tuli, "*Essentials of physical chemistry", 26th edition, S. Chand Publications, New Delhi*: 963, 2018.

[2] P. M. A. Khan, and M. Farooqui, "Analytical applications of plant extract as natural pH indicator: A review", *Journal of Advanced Scientific Research,* vol. 2, no. 4, pp. 20-27, 2011.

[3] K. A. Sajin, K. I. Anoobkumar, and O. K. Rasa, "pH Indicators: A valuable gift for analytical chemistry", *Saudi Journal of Medical and Pharmaceutical Sciences*, vol. 6, no. 5, pp. 393-400, 2020.

[4] H. Kahlert, G. Meyer, and A. Albrecht, "Colour maps of acid-base titrations with colour indicators: How to choose the appropriate indicator and how to estimate the systematic titration errors", *Chemistry Texts*, vol. 2, no.2, pp. 7-35, 2016.

[5] Y. Yang, J. Zhang, J. Yin, and Y. Yang, "Fast simultaneous determination of eight sudan dyes in chili oil by ultra-high-performance supercritical fluid chromatography", *Journal of Analytical Methods in Chemistry*, vo. 2019, Article ID 3731028, 2019.

[6] S. S. Mousavi, B. Sajad, B. Efafi, H. Alaibakhsh, K. E. Jahromi, M. H. Majlesara, and B. Ghafary, "Practical optimization of highly sensitive azo photoconductor with circular electrode scheme", *Journal of Lightwave Technology*, vol. 36, no. 24, pp. 5800-5806, 2018.

[7] Y. Ma, H. X. Chen, F. Zhou, H. Li. H. Dong, Y. Y. Li, Z. J. Hu, Q. F. Xu, and J. M. Lu, "Metal complex modified azo polymers for multilevel organic memories", *Nanoscale*, vol. 7, no. 17, pp. 7659-7664, 2015.

[8] A. J. Manaf and G. S. Athra, "Preparation and characterization of two azo dyes For dibenzothiophen by the diazotization reaction and studying their action as acid-base indicators", *Journal of University of Anbar for Pure Science*, vol. 7, no. 2, pp. 57-63, 2013.

[9] R. H. Fayadh, A. Ali, and M. Al-J. Fatima, "The synthesis and identification azo dyes derived from mercuried sulfa compounds and used their as indicator of acid-base", *Research Journal of Pharmaceutical, Biological and Chemical Sciences*, vol. 6, no. 3, pp. 1278-1285, 2015.

[10] M. H. Suaad, and G. A. Mohammed, "Synthesis and characterization of new azo compounds linked to 1,8-naphthalimide and studying their ability as acid-base indicators", *Iraqi Journal of Science*, vol. 60, no.11, pp. 2341-2352, 2019.

[11] A. A. Ali, "Synthesis and spectro analytical studies of a new azo dye derived from 2-amino-6 -ethoxybenzothiazole and 4-chloro-3,5-dimethylphenol and its complexes with Fe(III)ion", *Ibn Al-Haitham Journal for Pure and Applied Science*, vol. 27, no. 1, pp. 196-211, 2014.

[12] D. V. Snigur, A. N. Chebotarev, and K. V. Bevziuk, "Acid-base properties of azo dyes in solution studied using spectrophotometry and colorimetry", *Journal of Applied Spectroscopy*, vol. 85, pp. 21-26, 2018.

[13] A. H. Noor and A.K. Abbas, "Synthesis, spectroscopic characterization and thermal study of some transition metal complexes derived from caffeine azo ligand with some of their applications", *Eurasian Chemical Communication*, vol. 4, pp. 66-92, 2022.

[14] J. J. Duaa and A. K. Abbas, "Synthesis, identification, antibacterial, medical and dying performance studies for azo sulfamethoxazole metal complexes", *Eurasian Chemical Communication*, vol. 4, pp. 16-40, 2022.

[15] A. K. Abbas, and W.W. AL-Qaysi, "Synthesis and characterization of novel nano azo compounds using as a new acid indicator and pH sensors", *Arabian Journal for Science and Engineering*, vol. 48, pp. 399-415, 2023.

[16] A. Natansohn, and P. Rochon, "Photoinduced motions in azo-containing polymers", *Chemical Reviews*, vol. 102, no.11, pp. 39-76, 2002.

[17] G. Stela, B. Artem, G. Anton, and V. Marian, "Complex activity and sensor potential toward metal ions in environmental water samples of N-phthalimide azo-azomethine dyes", *Molecules*, vol. 26, no.19, p. 5885, 2021.

[18] K. Vivekshinh, K. Bharti, and G. Nidhi, "A new azo dye based sensor for selective and sensitive detection of Cu(II), Sn(II), and Al(III) Ions", *Biological and Medicinal Chemistry*, 2021.

[19] N. M. Mallikarjuna and J. Keshavayya, "Synthesis, spectroscopic characterization and pharmacological studies on novel sulfamethaxazole based azo dyes", *Journal of King Saud University-Science*, vol. 32, no. 1, pp. 251-259, 2020.

[20] A. K. Abbas, "Synthesis, spectroscopic, thermal and biological studies of some novel metal ions complexes", *International Journal of Applied Sciences and Technology*, vol. 4, no. 3, Article ID 187, 2022.

[21] N. A. Hussein and A. K. Abbas, "Synthesis, spectroscopic characterization and thermal study of some transition metal complexes derived from caffeine azo ligand with some of their applications", *Eurasian Chemical Communication*, vol. 4, pp. 66-92, 2022.

[22] A. K. Abbas, "Lanthanide ions complexes of 2-(4-aminoantipyrine)-L-tryptophane (AAT): preparation, identification and antimicrobial assay", *Iraqi Journal of Science*, vol. 56, no. 4C, pp. 3297-3309, 2015.

[23] A. K. Abbas, "Preparation, characterization and biological evaluation of some lanthanide (III) ions complexes with 3-(1-methyl2-benzimidazolyl azo)-Tyrosine", *Baghdad Science Journal*, vol. 13, no. 2, pp. 128-142, 2015

[24] N. Mallikarjuna, J. Keshavayya, M. Maliyappa, R. S. Ali, and T. Venkatesh, "Synthesis, characterization, thermal and biological evaluation of Cu(II), Co(II) and Ni(II) complexes of azo dye ligand containing sulfamethaxazole moiety", *Journal Molecular Structure*, vol. 1165, pp. 28-36, 2018.

[25] X. Zhou, Y. Du, and X. Wang, "Azo polymer janus particles possessing photo deformable and magnetic field responsive dual functions", *Chemistry -An Asian Journal*, vol. 11, no. 15, pp. 2130-2134, 2016.

[26] F. A. Noor and A. K. Abbas, "Novel complexes of thioarbituric acid –azo dye: structural, spectroscopic, bioogica activity and dying", *Biochemistry Cellular Archives*, vol. 20, no. 1, pp. 2419-2433, 2020.

[27] E. N. Masten, A. G. Fox and M. A. Keefe, "International tables for crystallography", *Kluwer Acadmic, Dordrect*, 2004.

[28] M. S. Masoud, A. E. Ali, S. G. Elasala, and S. A. Kolkaila, "Spectroscopic studies and thermal analysis on cefoperazone metal complexes", *Journal of Chemical and Pharmaceutical Research*, vol. 9, no.4, pp. 171-179, 2017.

[29] D. J. Jasim and A. K. Abbas, "Divalent metal complexes of azo sulfamethaxazole, Synthesis and characterization with study some of their applications", *Natural Volatiles Essential Oils Journal*, vol. 8, no. 4, pp. 8272-83300, 2021.